# Lateral torsional buckling capacity of steel beams with tapered web: FEA vs AISC(DG-25)

Mahmoud Magdy, Ali Hammad, Ahmed A. Matloub, Sherif M. Ibrahim

**Abstract**— Steel beams with tapered web often provide preferred option than web with constant depth duo to their higher strength to weight ratio which is better to resist variable moment along the beam. AISC Design Guide 25 (Frame Design Using Nonprismatic Members) offers provisions for the stability verification of members with tapered web. In this paper, the provisions of AISC Design Guide 25 regarding the lateral torsional buckling are firstly discussed in summarized steps. After that, the results are studied and validated against finite element analysis (FEA). The proposed FEA was built to simulate the behavior of steel beams under bending and having tapered web. Both material and geometrical imperfections were considered in the FEA. The FEA was verified using published numerical and experimental results, then a parametric study was carried out including the change of tapering ratio and beam length for different cross-section properties. Results of moment capacity from FEA are extracted and compared with AISC Design Guide 25 for the different studied cases. The conclusions of this comparison are presented.

**Index Terms** — Tapered section, bending moment, lateral torsional buckling.

## 1 Introduction

Members having tapered web are commonly used in the steel building. They are used for beams and columns subject to gradient moment providing a distinguished solution compared to traditional members with constant depth. This efficient solution is adopted by adjusting the depth of the members to the bending moment distribution along the length leading to an economical solution.

Laterally unsupported members are susceptible to out-of-plane buckling when subject to compression, while they are susceptible to lateral torsional buckling (LTB) when subject to bending. The resistance of laterally unsupported beams depends on both elastic LTB strength and cross-section properties.

For beams having tapered web, LTB verification was addressed in international specifications. American specification (AISC) provides design specification for steel structures, in addition to design guidelines for other different aspects related to special conditions that not covered in the specification. One of them, AISC Design Guide 25, addressed the design of members having tapered web.

AISC(DG-25), last edition, is a modified version of the AISC provisions to take into consideration the influence of nonprismatic geometry. The main difference between the last edition and the previous one is the account for the bending stresses in the calculations instead of the bending moments to deal with tapered beams.

Earlier editions of AISC steel design code till (AISC LRFD, 1993) [1] included provisions for the design of members having tapered web. However, the latest edition of AISC specifications (ANSI/AISC 360-16, 2016) removed the provisions for the LTB of the members with tapered web. These provisions were separately issued in the AISC design guides.

AISC(DG-25_2011) [2] is the first edition for the design of tapered members. There is another updated edition published recently, AISC(DG-25_2021) [3]. The provisions of AISC(DG-25) for LTB are modified versions of the AISC provisions to account for the influence of non-prismatic member geometry.

The two previous editions have many differences specially in the calculation of lateral torsional buckling resistance of the tapered steel beams. In this paper, a study was conducted to validate the LTB moment capacity provisions of AISC(DG-25), second edition. The validation was conducted using verified FE models.

## 2 Literature Review

Beams having tapered web were used in steel construction for many years. A lot of experimental, analytical and numerical investigations on the beams with tapered web have been conducted to study their behavior. Kitipornchai and Trahair [4] put the first theoretical basis for the LTB of tapered beams. Prawel et al. [5] introduced experimental work to study the inelastic behavior of tapered sections subject to moment and compression. Shiomi and Kurata [6] presented also experimental work on beams with tapered web subject to gradient moment to investigate the lateral torsional buckling. They extended their work using numerical study. Braham & Hanikenne [7] proposed a practical method to calculate LTB buckling strength of beams with tapered web. Andrade and Camotim [8] studied cantilever beams having tapered web and proposed a solution for the critical load acting at the tip of the cantilever. The last solution covered the elastic critical load; however, Andrade et al. [9] continued the work to include the pre-buckling deformations in the calculation. Zhang and Tong [10] proposed an equivalent section properties to be used for calculating the LTB capacity of the beams with tapered web. On the other hand,


- *Mahmoud Magdy, MSc Candidate, Struct. Eng. Department, Ain Shams University, Egypt. (mahmoudmagdi@eng.asu.edu.eg)*
- *Ali Hammad, Assistant Professor, Struct. Eng. Department, Ain Shams University, Egypt. (ali.hammad@eng.asu.edu.eg)*
- *Ahmed A. Matloub, Assistant Professor, Struct. Eng. Department, Ain Shams University, Egypt. (ahmed.matloub@eng.asu.edu.eg)*
- *Sherif M. Ibrahim, Professor, Struct. Eng. Department, Ain Shams University, Egypt. (sherif_ibraim@eng.asu.edu.eg)*


IJSER

Kim [11] proposed a simplified procedure to calculate the capacity which was issued in AISC(DG-25_2011) [2]. In continuation, Marques et al. [12] proposed another design procedure for beams with tapered web to account for the lateral torsional buckling. The studies on beams with tapered web continued through different publications, e.g. Tankova et al. [13], Kucukler and Gardner [14], Quan et al. [15], until issuing the second edition of design guide AISC(DG-25_2021) by White et al. [3].

It is obvious that there are many studies were conducted on the behavior and design of beams with tapered web, and the design guide related to same topic is dynamic with recent update. In this paper FEA is used to verify the last issue of the design guide.

## 3 Verification

The finite element analysis is a tool that can provide a dependable result on different studies. The FEA is used here to verify the calculation of the design guide of beams having tapered web. FEA is first verified with available previous results issued by Prawel et al. [5] and Kim [11]. ABAQUS CAE software v6.14 is used in this paper.

The dimensions of beam's cross-sections as given by Prawel et al. [5] are shows in Table 1, while the FEA created in this paper is presented in Fig. 1. The beams are hinged-roller beams to simulate simply supported condition. The models are loaded at one-quarter and three-quarter the span. Stiffeners are used at the supports and the loaded points. For tests LB-3 and LB-5, the top and bottom flanges are laterally restrained at the supports and at the load points. Also, the load at the shallower depth is 28% of the load at the deeper depth. The condition of LB-6 is similar, but the load is only one load applied at the deeper depth with no lateral restraint at the unloaded point.

IJSER

Table 1 Geometric characteristics of studied beams

| Test | β (°) | L (m) | bf (mm) | $t_w$ (mm) | $t_f$ (mm) | $d_s$ (mm) | $d_L$ (mm) |
|---|---|---|---|---|---|---|---|
| LB-3 | 3.97 | 3.66 | 101.6 | 2.67 | 6.35 | 152.4 | 406.4 |
| LB-5 | 5.95 | 2.44 | 101.6 | 2.67 | 6.35 | 152.4 | 406.4 |
| LB-6 | 5.95 | 2.44 | 101.6 | 2.67 | 6.35 | 152.4 | 406.4 |

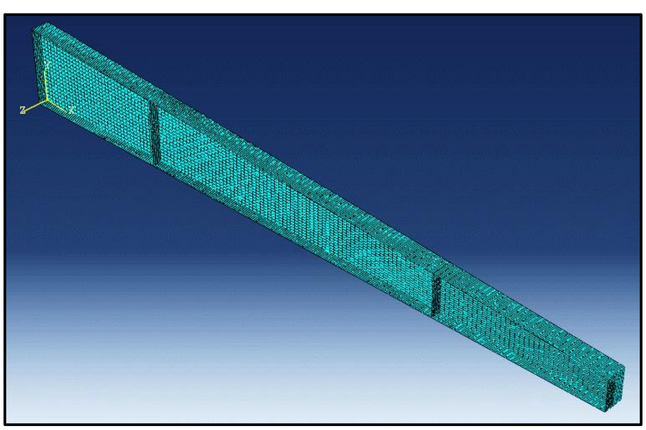

Fig. 1 Finite element analysis

Shell element is used to simulate the beam including its flanges and web, also the stiffeners. The element is four nodes at the corners only with reduced integration. It is denoted in the software as S4R. The mesh size is selected around 50 mm and distributed to adopt aspect ratio of the element between 1 and 2.

Prawel et al. [5] reported that the measured yield strength of the tested beams were 52ksi (360Mpa) as a results of the coupon tests. As reported by Kim [11], it is expected that thinner plates of web should larger yield strength that of flanges. The yield strength of the web panel was taken 450Mpa for the beam tests LB-5 and LB-6 to eliminate the predominant shear failure mechanism in the virtual test simulation in the end panels as recommended by Kim [11]. The constitutive material model is adopted as linearly elastic with strain hardening using the true stress-strain relationship.

The FEA include advanced numerical simulation with geometrical and material imperfection. The initial geometric imperfections were modelled by conducting a linear buckling analysis and scaling the mode shape to a limit of $L_b/1000$. The target mode in our case was the sweep of the compression flange. The target mode shape of the tested beams is shown in Fig. 2.

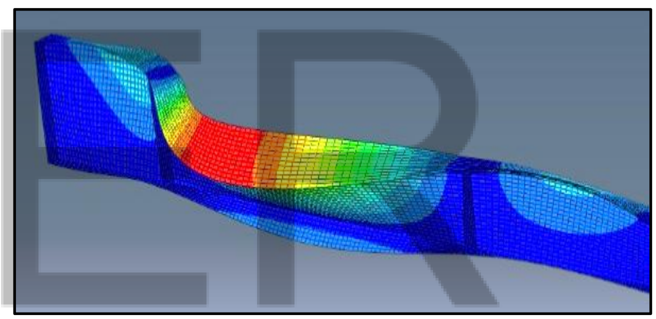

Fig. 2 Mode shape of tested beams

For the residual stresses, Kim [11] studied four different residual stresses patterns and recommended to use the best-fit residual stress pattern as shown if Fig. 3. The selected pattern must be self-equilibrating for each cross-section component. It was modelled using the ABAQUS *INITIAL CONDITIONS option with TYPE=STRESS, USER. The user defines the initial stress value in a * STATIC step with no loading to allow for equilibrating of the initial stress field before starting the response history.

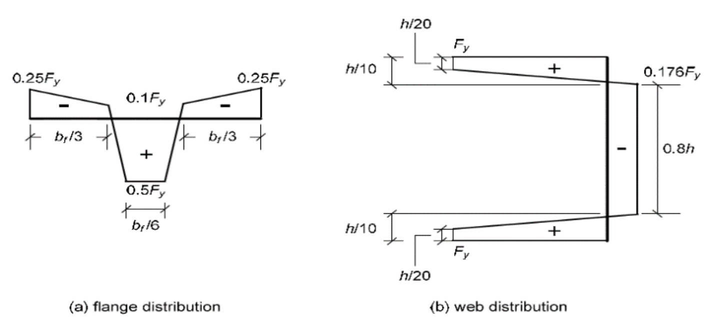


Fig. 3 Nominal residual stress pattern

A comparison between load and displacement measured by Prawel et al. [5] and that extracted from the proposed FEA is conducted. The mode of failure of the proposed FEA has detected to have the same mode of failure of the experimental test for all specimens. The failure modes of the different models using the proposed FEA are presented in Fig. 4.

A further comparison is presented between the load capacity from the experimental results Prawel et al. [5], the proposed FEA in this paper, the results obtained by Kim [11], and the results from the provisions of AISC(DG-25_2021) [3]. The results are summarized in Table 2. For LB-3, it is obvious that the experimental result is higher than the expected one for member having the same geometric characteristics as discussed by Kim [11]. For LB-5, the shear tension field action is dominant at the maximum load. In general, the FEA in this paper is found identical with Kim [11], also they are in a good relationship with both the experiments by Prawel [5] and DG-25.

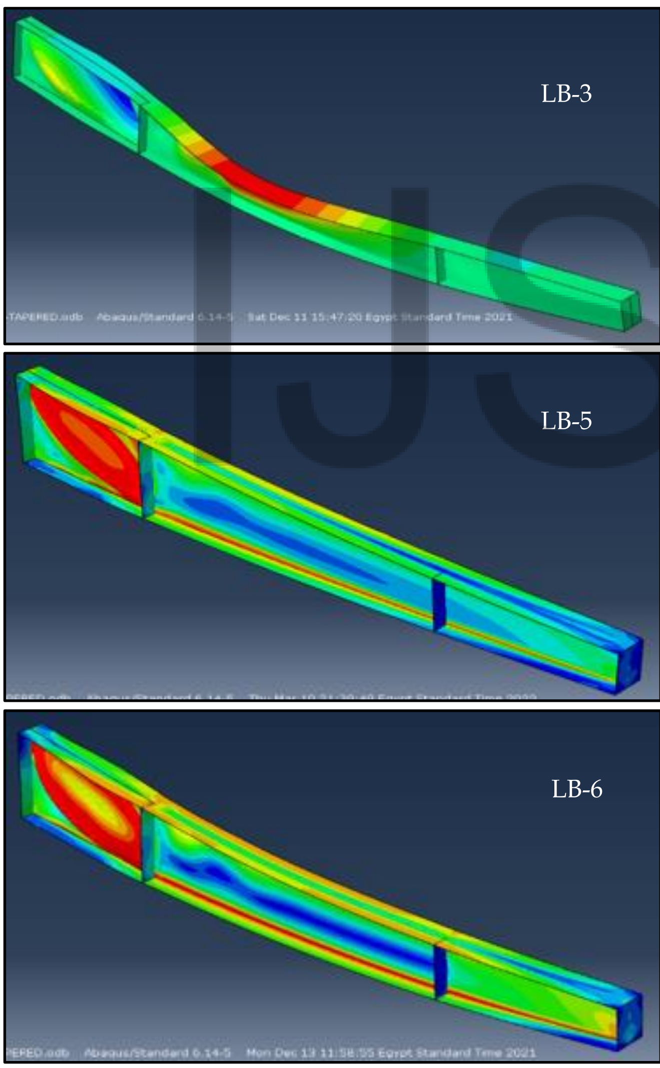

Fig. 4 Failure mode of specimens LB-3, LB-5, and LB-6 of proposed FE models

Table 3
Comparison between experimental results [5], results obtained by Kim [11], results obtained from proposed FEA, and results from AISC(DG-25_2021) [3]

| beam | Exp. test (kN) | Kim [11] (kN) | FEA (kN) | DG-25 (kN) |
|---|---|---|---|---|
| LB-3 | 136 | 108 | 111 | 102 |
| LB-5 | 174 | 164 | 164 | 174 |
| LB-6 | 205 | 179 | 182 | 209 |

## 4 AISC(DG-25) LTB PROVISIONS

In this section, the existing provisions of LTB in AISC(DG-25) [3] will be studied. The used provisions are applied for the estimation of LTB for unbraced lengths having prismatic flanges and single linear web taper subjected to single curvature bending. Break down for the calculation is summarized as follows:

1- Calculate the compressive bending stress ($F_r$) and the elastic LTB stress ($F_{e,LTB}$) at different cross sections locations, (beams' ends, one-quarter, middle, three-quarter and at the maximum moment), as follows:

$$F_r = \frac{M}{S_x} \tag{1}$$

$$F_{e,LTB1} = \frac{\pi^2 E}{\left(\frac{L_b}{r_t}\right)^2} \sqrt{1 + 0.078 \frac{J}{S_{xc} h_0} \left(\frac{L_b}{r_t}\right)^2} \tag{2}$$

Where M is the bending moment at the studied cross-section, $S_x$ is the elastic section modulus about the major axis, E is modulus of elasticity of steel, $L_b$ is the length between unbraced point against lateral displacement of the compression flange, J is St. Venant torsional constant as $J = \sum bt^3 / 3$, $h_o$ is the distance between the flange centroids, $S_{xc}$ is the elastic section modulus about the major axis of the compression side, $r_t$ effective radius of gyration for LTB and can be approximated conservatively as the radius of gyration of the compression flange plus one-sixth of the web

$$r_t = \frac{b_f}{\sqrt{12\left(1 + \frac{1}{6}\frac{h t_w}{b_f t_f}\right)}}$$

2- Determine the moment gradient factor ($C_b$) as

$$C_b = \frac{4\left(\frac{F_r}{F_{e,LTB1}}\right)_{max}}{\sqrt{\left(\frac{F_r}{F_{e,LTB1}}\right)_{max}^2 + 4\left(\frac{F_r}{F_{e,LTB1}}\right)_A^2 + 7\left(\frac{F_r}{F_{e,LTB1}}\right)_B^2 + 4\left(\frac{F_r}{F_{e,LTB1}}\right)_C^2}} \tag{3}$$

The subscripts A, B, and C denote the value of this ratio at one-quarter, middle and three-quarter point locations, respectively, within the unbraced length under consideration.

3- Calculate the elastic LTB load ratio, ($\gamma_{e,LTB}$), using $C_b = 1$, as

$$\gamma_{e,LTB} = \frac{C_b}{\left(\frac{F_r}{F_{e,LTB1}}\right)_{max}} \tag{4}$$

4- Calculate $F_L$ as $F_L = 0.7\ F_y$

5- At various locations along the unbraced length, determine which LTB range applies, then calculate the moment capacity ($M_n$) using the buckling load ratio, ($\gamma_{e,LTB}$), and the compression flange flexural stress at that location, ($F_r$):

a- If $\frac{Fr\ \gamma_{e,LTB}}{Fy} \geq \frac{\pi^2}{1.1^2} = 8.2 \rightarrow$ No LTB exist

b- If $8.2 > \frac{Fr\ \gamma_{e,LTB}}{F_y} > \frac{F_L}{F_y} \rightarrow$ Calculate the inelastic LTB strength as:

$$M_n = C_b R_{pg} R_{pc} M_{yc} \left[1 - \left(1 - \frac{F_L}{R_{PC} F_{yc}}\right)\left(\frac{\pi\sqrt{\frac{F_{yc}}{F_r \gamma_{e,LTB}}} - 1.1}{\pi\sqrt{\frac{F_{yc}}{F_L}} - 1.1}\right)\right] \le R_{pg} R_{pc} M_{yc} \quad (5)$$

Where $R_{pc}$ is the web platification factor, cross-section effective shape factor limited by compression, $R_{pg}$ is the bending stress reduction factor which is equal to 1.0 for sections with compact or non-compact webs and less than 1.0 for sections with slender webs.

c- If $\frac{F_r \gamma_{e,LTB}}{F_y} \le \frac{F_L}{F_y}$ → calculate the elastic LTB strength as:

$$M_n = C_b R_{pg} \gamma_{e,LTB} F_r S_{xc} \le R_{pg} M_{yc} \quad \text{(for slender web)} \quad (6)$$

$$M_n = C_b \gamma_{e,LTB} F_r S_{xc} \le R_{pc} M_{yc} \quad \text{(for other members)} \quad (7)$$

6- The LTB strength ratio for the entire unbraced length is the largest ratio of $M/M_n$ calculated at different critical cross sections along the unbraced length.

The previous equations are presented with the concentration on our studied cases. It's clear that AISC(DG-25) [3] provide a practical method to calculate the LTB strength of web-tapered steel beams.

## 5 Verification of DG-25 using FEA

After the verification of the FEA, a study was conducted using FEA to validate the accuracy of the recent issue of the design guide AISC(DG-25_2021) [3]. A comparison between LTB moment capacity from FEA and the capacity from AISC(DG-25) [3] is concluded in this section.

The studied beams are simply supported beams having tapered web and flanges with constant width. The sections are built-up sections welded from steel plates to form I-shape. This type of fabrication is the main process used in forming the beams with tapered web. Taking reference from common sections, the dimensions of the section having shallower depth were taken equal to European standard hot-rolled I-sections. In addition, the dimensions of the section having deeper depth were taken the same width of flange and the same thickness of both flange and web, while the web depth is multiplied by 1.0 to 4.0. All beams are subject to concentrated moment at both ends with same magnitude and inverse direction to simulate constant moment along the beam length. The beam lengths were changed for taken as 4.0 m up to 14.0 m.

Fig. 5 presents the relationship between the normalized on the vertical axis and the tapering ratio on the horizontal axis for three different profiles and three different spans. The normalized moment is calculated by dividing the FEA moment of the tapered section, $M_n$, by the FEA moment of the beam with constant depth using the shallower web, $M_{n,0}$. The same is also presented in the figure using the results of the design guide. For IPE sections, the length was taken equal to 8m. For HEA and HEB beams, the length was taken equal to 12m.

It is obvious from the charts that the results of AISC(DG-25) is almost in a good agreement with FEA for most cases. The FEA gives higher moment than the design guide with difference 2% to 5% for all cases with wide flanges (HEA and HEB sections). For the case of flanges with smaller width (IPE sections), it is noticeable that the moment resistance according to the design guide is more conservative especially for cases of high tapering ratio. The difference between FEA and DG-25 increases as the tapering ratio increases, reaching a maximum value of 13% for beam having the deeper depth equal to four times the shallower depth.

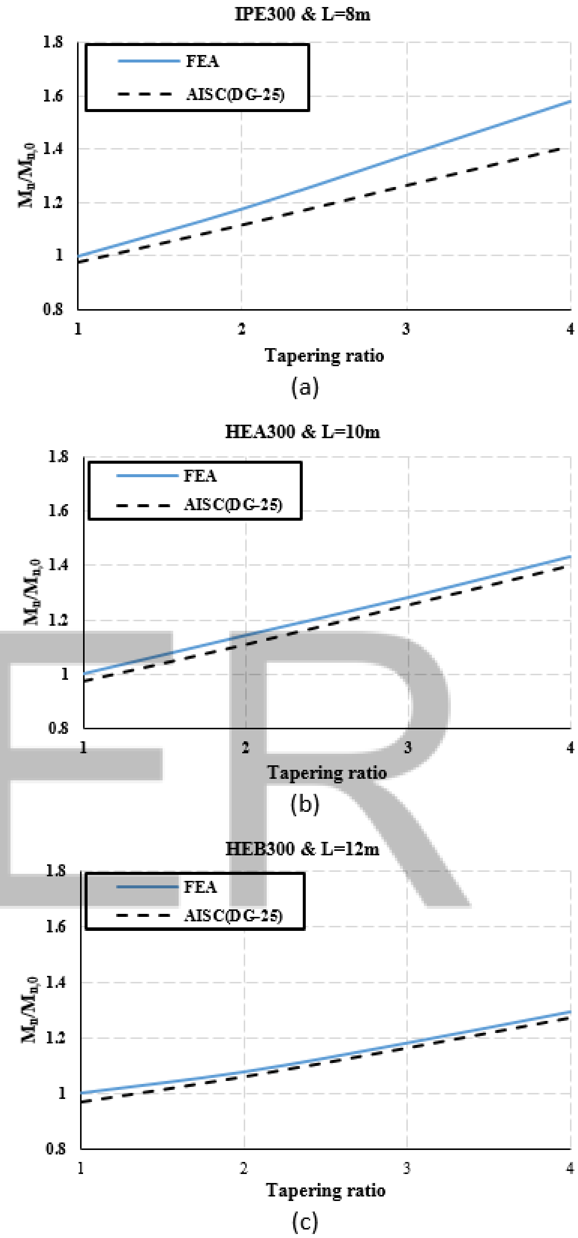


Fig. 5 Comparison between FEA and DG-25 regarding the tapering ratios for different profiles and different spans

To investigate the previous results with different lengths, Fig. 6 is presented. The figure shows the relationship between normalized moment on the vertical axis and the beam length on the horizontal axis for three different profiles. The tapering ratio is taken constant, equal to 3.0. The normalized moment is calculated by dividing FEA moment of the tapered beam, $M_n$, by the yielding moment, $M_y$, calculated at the section having shallower depth. The same is also presented in the figure using the results of the design guide.

The same result is noticed from the figure. The FEA gives values very close to the one from the design guide. The com-

IJSER

mon trend of the curves is detected showing a yielding behavior at the beginning for beams with small length. Then, the trend follows the conventional lateral torsional buckling for beams with large lengths. This is noticed for wide flange profiles (HEA and HEB), while for IPE sections the curve follows LTB from the beginning. The results between FEA and DG-25 are almost identical with small differences in case of wide flanges (HEA and HEB sections). The difference for case of IPE section is relatively high specially for longer beams, reaching 28% for case of 12.0 m length.

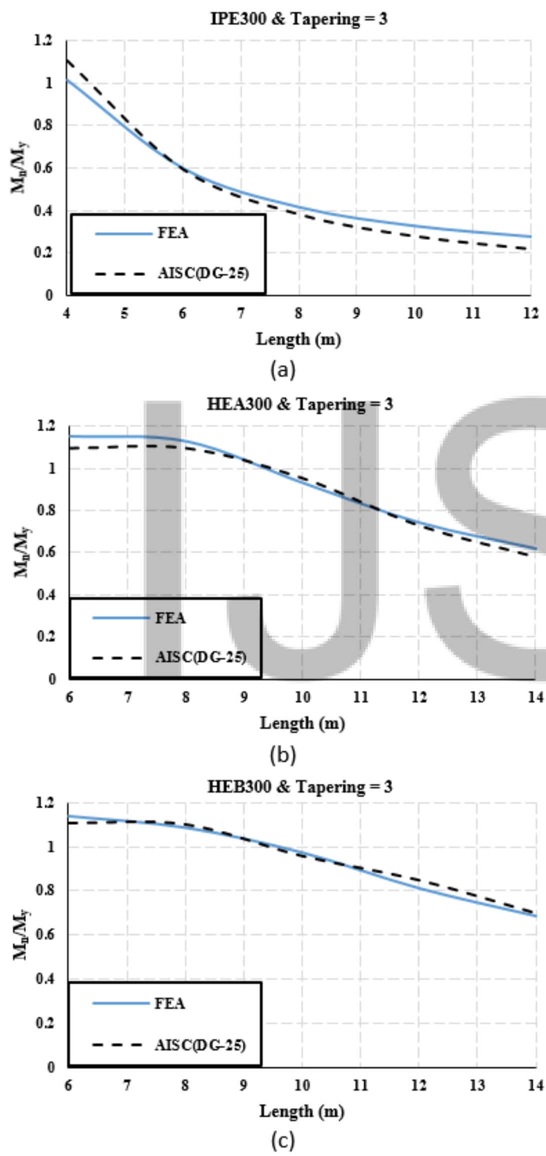


Fig. 6 Comparison between FEA and DG-25 regarding the beam length for different profiles

## 6 Conclusions

This paper validated the AISC(DG-25_2021) provisions of LTB for steel beams having tapered web using a verified FEA. The following conclusions are drawn from the results.

1. LTB moment capacity calculated from AISC(DG-25) [3] is in a good agreement with FEA results in most studied cases.
2. AISC(DG-25_2021) provides a practical and simple method to calculate the LTB moment capacity of beams with tapered web.
3. The agreement is clear for profiles with wide flanges; however, the profiles with narrow flanges show less agreement.
4. The gap for the profiles with narrow flanges is more wide with the increase of the beam length.

## 7 References


[1] American Institute of Steel Construction, *AISC LRFD Specification (1993).*, no.1. Chicago: American Institute of Steel Construction, 1998.

[2] R. C. Kaehler, D. W. White, and Y. D. Kim, *Frame design using web-tapered members*. American Institute of Steel Construction, 2011.

[3] R. S. Donald W. White , Woo Yong Jeong, *Frame Design Using Nonprismatic Members, AISC/MBMA Design Guide 25, 2nd Ed.* American Institute of Steel Construction, 2021.

[4] S. Kitipornchai and N. S. Trahair, “Elastic stability of tapered I-beams,” *J. Struct. Div.*, vol. 98, no. 3, pp. 713–728, 1972.

[5] S. P. Prawel, M. L. Morrell, and G. C. Lee, “Bending and buckling strength of tapered structural members,” *Weld. Res. Suppl.*, vol. 53, pp. 75–84, 1974.

[6] H. Shiomi and M. Kurata, “Strength formula for tapered beam-columns,” *J. Struct. Eng.*, vol. 110, no. 7, pp. 1630–1643, 1984.

[7] M. Braham and D. Hanikenne, “Lateral buckling of web tapered beams: An original design method confronted with a computer simulation,” *J. Constr. Steel Res.*, vol. 27, no. 1–3, pp. 23–36, 1993.

[8] A. Andrade and D. Camotim, “Lateral--torsional buckling of singly symmetric tapered beams: theory and applications,” *J. Eng. Mech.*, vol. 131, no. 6, pp. 586–597, 2005.

[9] A. Andrade, D. Camotim, and P. B. Dinis, “Lateral-torsional buckling of singly symmetric web-tapered thin-walled I-beams: 1D model vs. shell FEA,” *Comput. \& Struct.*, vol. 85, no. 17–18, pp. 1343–1359, 2007.

[10] L. Zhang and G. S. Tong, “Lateral buckling of web-tapered I-beams: A new theory,” *J. Constr. Steel Res.*, vol. 64, no. 12, pp. 1379–1393, 2008.

[11] Y. D. Kim, *Behavior and design of metal building frames using general prismatic and web-tapered steel I-section members*. Georgia Institute of Technology, 2010.

[12] L. Marques, L. S. da Silva, R. Greiner, C. Rebelo, and A. Taras, “Development of a consistent design procedure for lateral--torsional buckling of tapered beams,” *J. Constr. Steel Res.*, vol. 89, pp. 213–235, 2013.

[13] T. Tankova, J. P. Martins, L. S. da Silva, L. Marques, H. D. Craveiro, and A. Santiago, “Experimental lateral-torsional buckling behaviour of web tapered I-section steel beams,” *Eng. Struct.*, vol. 168, pp. 355–370, 2018.

[14] M. Kucukler and L. Gardner, “Design of web-tapered steel beams against lateral-torsional buckling through a stiffness reduction method,” *Eng. Struct.*, vol. 190, pp. 246–261, 2019.

[15] C. Quan, M. Kucukler, and L. Gardner, “Design of web-tapered steel I-section members by second-order inelastic analysis with strain limits,” *Eng. Struct.*, vol. 224, p. 111242, 2020.


IJSER